

Electronic Supplementary Information (ESI)

Exploring the gelation and AIE property of tripodal acylhydrazone-based probe: Turn-on Zn(II) sensing in HEPES buffer

Rubi Moral and Gopal Das*

Department of Chemistry, Indian Institute of Technology Guwahati, Assam, 781039, India;

Email: gdas@iitg.ac.in

S1. General Information and Materials. All the reagents for synthesis were purchased from Sigma-Aldrich Chemical Co. and used without further purification. PerkinElmer Lambda-25 UV-vis spectrophotometer was used for the measurement of the absorption spectra in the wavelength range of 250–800 nm, using 10 mm path-length quartz cuvettes. Horiba Fluoromax-4 spectrofluorometer was employed for fluorescence measurements keeping a slit width of 5 nm at 298 K, using 10 mm path-length quartz cuvettes. All the mass spectra were recorded using a Waters Q-ToF Premier mass spectrometer. Bruker Advance 600 MHz instrument was used to record Nuclear magnetic resonance (NMR) spectra, where the chemical shifts were recorded in parts per million (ppm) scale. To describe the spin multiplicities in the ^1H NMR spectra following abbreviations have been used: singlet: s; doublet: d; triplet: t, quartet: q, and multiplet: m. The morphology of the aggregated species was investigated by using FESEM imaging studies by the drop (1 mM) cast method on glass plates covered with Al-foil using Gemini 300 FESEM (Carl Zeiss) and Sigma 300 FESEM (10000KX).

S2. Synthesis of TRI-NH₂. TRI-NH₂ was synthesized using the procedure described in previous literature.¹ Benzene-1,3,5-tricarboxylic acid (1g) was placed in a 50 mL round-bottomed flask and dissolved in ethanol (EtOH) (30 mL). A few drops of concentrated H₂SO₄ were added to the flask. The reaction was refluxed at 74 °C for 48 hours. The precipitates were separated by filtration and washed with EtOH (30 mL). The obtained white crystalline product (500 mg) was dried and taken in a round-bottomed flask for further reaction with an excess amount of hydrazine hydrate (NH₂NH₂·H₂O). The reaction was refluxed at 74 °C for 24 hours. The white precipitates were separated by filtration washed with EtOH (30 mL) and vacuum dried to obtain TRI-NH₂. ^1H NMR [600 MHz, DMSO-*d*₆, δ (ppm)]: 3 \times [9.85 (s, 1H), 8.32 (s, J = 2.2 Hz, 1H), 4.58 (s, 2H)]. ^{13}C NMR [151 MHz, DMSO-*d*₆, δ (ppm)] 165.47 \times 3, 134.31 \times 3, 128.51 \times 3.

S3. Synthesis of Probe TRI-QUI. TRI-NH₂ (200 mg, 0.793 mmol, 1 equiv.) was placed in a 50 mL round-bottomed flask and dissolved in ethanol (EtOH) (10 mL). 8-quinoline carboxaldehyde (436 mg, 2.80 mmol, 3.5 equiv.) was added and the reaction was refluxed at 74 °C for 24 hours. The precipitates were separated by filtration and washed with EtOH (30 mL). The obtained white amorphous product was further vacuum-dried and isolated as compound TRI-QUI. It was further crystallized from DMSO and a suitable single crystal was isolated for SC-XRD analysis. Calculated yield: 95%. ^1H NMR [600 MHz, DMSO-*d*₆, δ (ppm)]: 3 \times [12.49 (s, 1H), 9.88 (s, 1H), 9.03 (d, J = 3.9 Hz, 1H), 8.85 (s, 1H), 8.51-8.45 (m, 2H), 8.15 (d, J = 7.8 Hz, 1H), 7.78 (t, J = 7.5 Hz, 1H), 7.67 (dd, J = 8.2, 4.0 Hz, 1H)]. ^{13}C NMR

[151 MHz, DMSO- d_6 , δ (ppm)]: 3 \times [162.41, 150.97, 146.01, 145.90, 137.24, 134.47, 131.50, 130.79, 130.62, 128.57, 127.13, 126.32, 122.47]. ESI-MS (positive mode, m/z) calculated for $C_{39}H_{27}N_9O_3$: 669.2237, found: 670.2327 [$M + H^+$]. Empirical formula $C_{39}H_{29}N_9O_4$, Mw: 687.71, $T = 297$ K, triclinic, space group: P-1, $a = 8.3334$ (12) Å, $b = 11.9948$ (17) Å, $c = 16.823$ (2) Å, $\alpha = 94.916$ (4) $^\circ$, $\beta = 99.085$ (4) $^\circ$, $\gamma = 94.038$ (4) $^\circ$, $V = 1648.3$ (4) Å³, $Z = 2$, D_x (g cm⁻³) = 1.386, $F(000) = 716.0$, total no. of reflections/no. of independent reflections/no. of observed reflections = 38298/5791/3398, R_1 , $I > 2\sigma(I) = 0.0824$ (3398), wR_2 , $I > 2\sigma(I) = 0.2981$ (5791), GOF (F_2) = 1.107. CCDC:: 2363554.

S4. Synthesis of Probe TRI-NAP. TRI-NAP was synthesized with a similar procedure as to that of TRI-QUI, where, TRI-NH₂ (200 mg, 0.793 mmol, 1 equiv.) was placed in a 50 mL round-bottomed flask and dissolved in N,N-Dimethylformamide (DMF) (10 mL). 1-naphthaldehyde (436 mg, 2.80 mmol, 3.5 equiv.) was added and the reaction was refluxed at 60 C for 24 hours. The clear yellow solution was poured into ice-cold water and the white precipitates obtained were separated by filtration and washed with distilled water (30 mL). The obtained white powder product was further vacuum-dried and isolated as compound TRI-NAP. Calculated yield: 80%. ¹H NMR [600 MHz, DMSO- d_6 , δ (ppm)]: 3 \times [12.36 (s, 1H), 9.22 (s, 1H), 8.88 (d, $J = 8.4$ Hz, 1H), 8.80 (s, 1H), 8.07 (dd, $J = 14.1, 8.6$ Hz, 2H), 8.02 (d, $J = 7.1$ Hz, 1H), 7.75 – 7.70 (m, 1H), 7.65 (m, $J = 12.0, 7.9$ Hz, 2H)]. ¹³C NMR [151 MHz, DMSO- d_6 , δ (ppm)]: 3 \times [162.51, 148.90, 134.77, 134.04, 131.30, 130.76, 130.39, 129.90, 129.36, 128.35, 127.95, 126.85, 126.13, 124.59]. ESI-MS (positive mode, m/z) calculated for $C_{42}H_3N_6O_3$: 666.2379, found: 667.2453 [$M + H^+$].

S5. UV-Vis- and Fluorescence-Spectroscopy Studies. Stock solutions of all the metal ions (using acetate, chloride, and nitrate salts) (50mM) were prepared in water. Stock solutions of all the anions (using *n*-Tetrabutylammonium salts of the corresponding anions) (50mM) were prepared in DMSO. Stock solutions of TRI-QUI (5×10^{-3} mol L⁻¹) and TRI-NAP (5×10^{-3} mol L⁻¹) were prepared in DMSO and then diluted to 10×10^{-6} mol L⁻¹ for various spectral studies by placing only 4.0 μ L of TRI-QUI or TRI-NAP stock solution into an aqueous medium to a final volume of 2.0 mL. In the fluorescence/UV-Vis sensing experiment, the test samples were prepared by placing the appropriate amounts of the stock solutions of the respective metal ions into 2.0 mL of probe solution (containing 10×10^{-6} mol L⁻¹ of probe and 0.2% DMSO). For fluorescence titration experiments, 5×10^{-3} mol L⁻¹ stock solution of Zn(OAc)₂.2H₂O (zinc acetate dihydrate), Cd(OAc)₂.2H₂O (cadmium acetate dihydrate), and HgCl₂ (mercuric chloride) was prepared in DMSO, then it was gradually added into a 2.0 mL

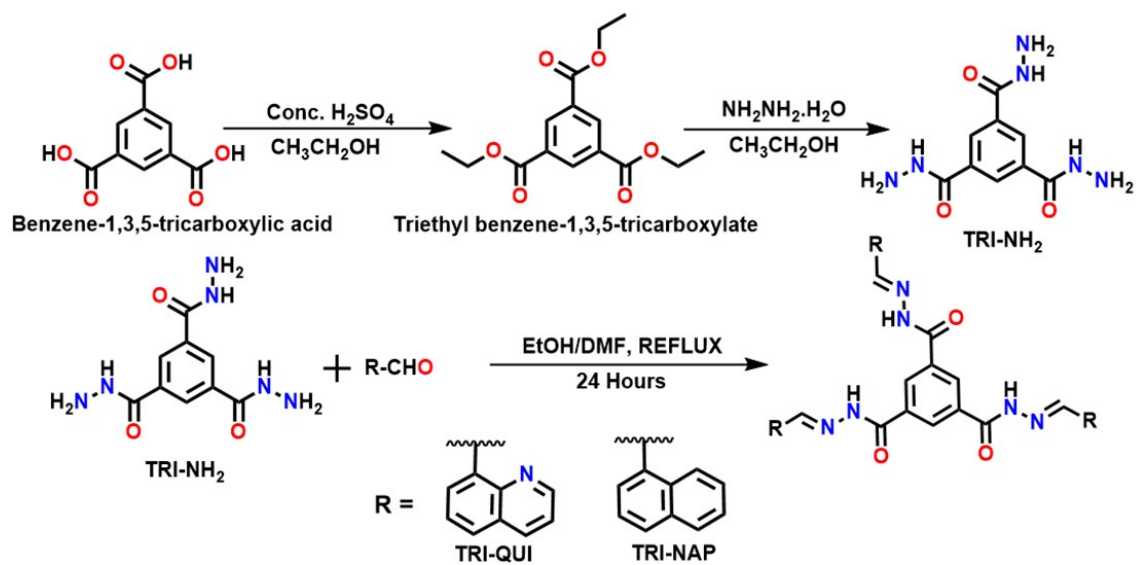
of probe solution (containing 10×10^{-6} mol L⁻¹ of probe and 0.2% DMSO) using a micropipette in a quartz optical cells with 1.0 cm path lengths.

S6. Detection Limit. Using a fluorescence titration experiment as a basis we calculated the detection limit. The standard deviation (σ) of blank measurement was estimated by measuring the fluorescence emission spectrum of **TRI-QUI** in water (five times) and HEPES (five times). Fluorescence emission values to the concentration of Zn²⁺ (obtained from fluorescence titration experiment) were plotted to measure the slope (k). The following equation was used to calculate the detection limit:

$$\text{Detection limit} = 3\sigma/k$$

Where, σ = standard deviation of blank measurement, and k = slope between the fluorescence emission intensity versus concentration of Zn²⁺.

S7. Crystallographic Refinement Details. For the probe **TRI-QUI** all the details of the hydrogen-bonding and noncovalent interactions are furnished in **Table S1**, and also all of the above given data have been deposited into CCDC. A suitable single crystal was selected and mounted into a loop. Supernova (a single source at an offset) Eos diffractometer with Mo K α radiation ($\lambda = 0.71073$ Å) source, connected with a CCD region detector was used to collect the X-ray intensity data, and all the data refinement and cell reduction were done by using APEX 3/APEX 4.^{2,3} Using a narrow-frame algorithm and XPREP, the frames were combined with the Bruker SAINT software kit,⁴ and data were corrected for absorption effects using the Multi-Scan process (SADABS)⁵. Using direct methods in XT, version 2014/15, all of the structures were solved and after that, refinement was done using the full-matrix least-squares technique in the SHELXL-2016 and 2018 software packages on F2.⁶ MERCURY 4.2.0 was used for creating structural drawings.⁷



Scheme S1. Synthesis of TRI-QUI and TRI-NAP.

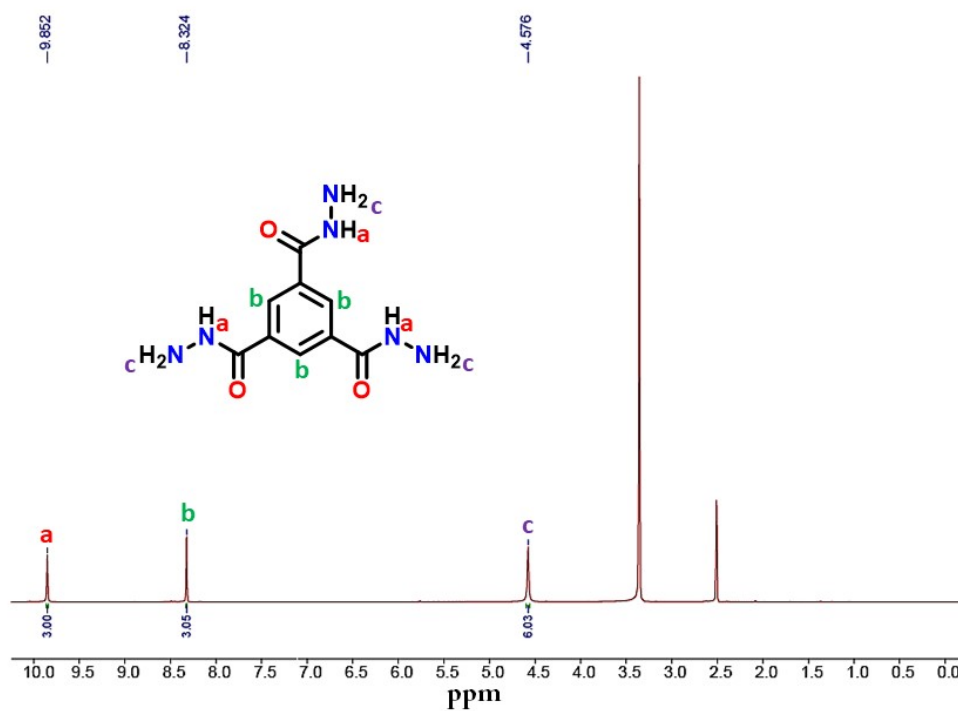


Figure S1. ¹H NMR spectrum of TRI-NH₂ in DMSO-*d*₆.

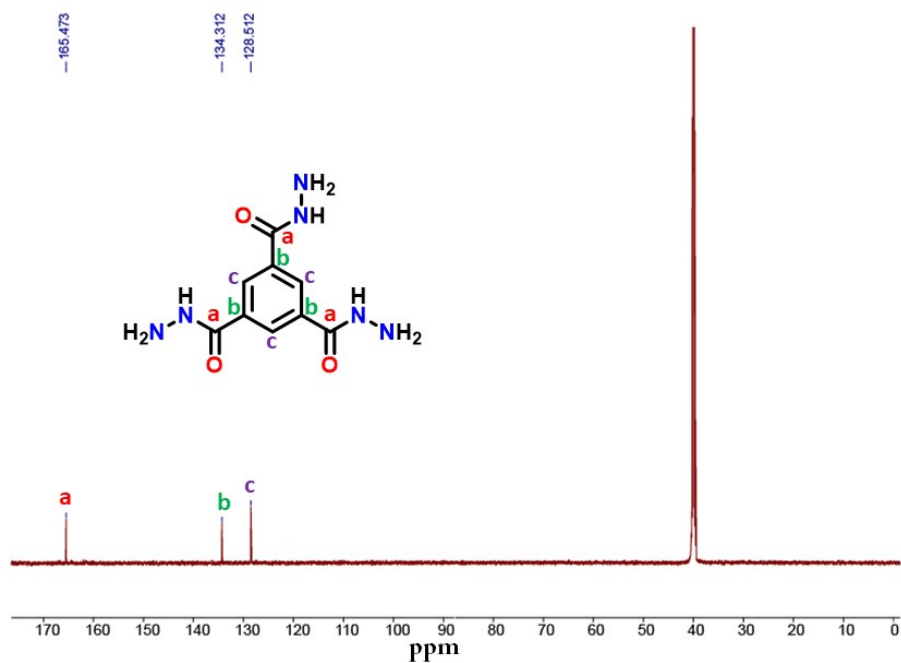


Figure S2. ¹³C NMR spectrum of TRI-NH₂ in DMSO-*d*₆.

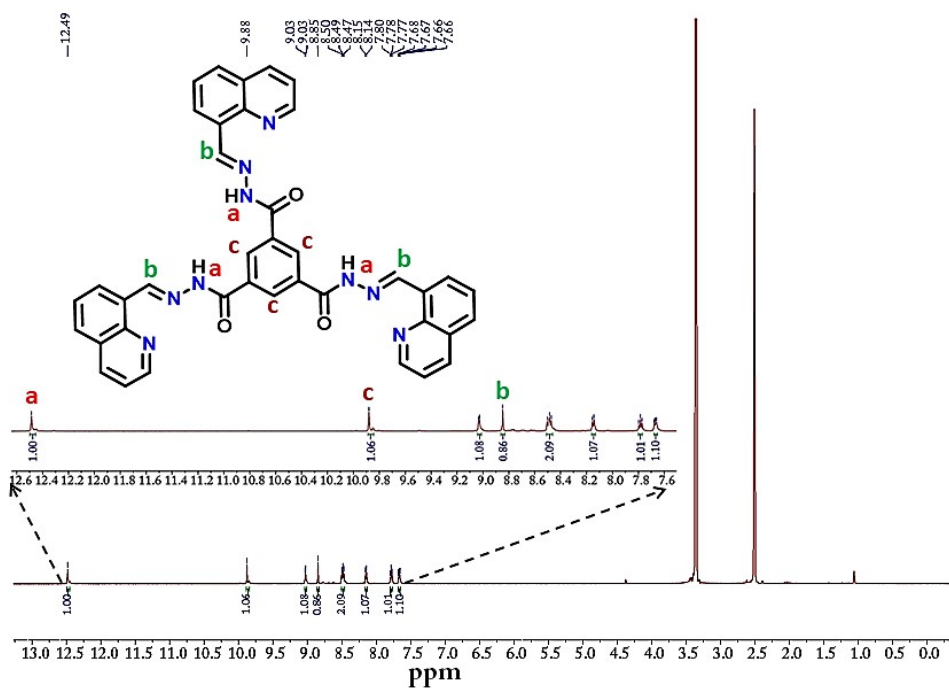


Figure S3. ¹H NMR spectrum of TRI-QUI in DMSO-*d*₆.

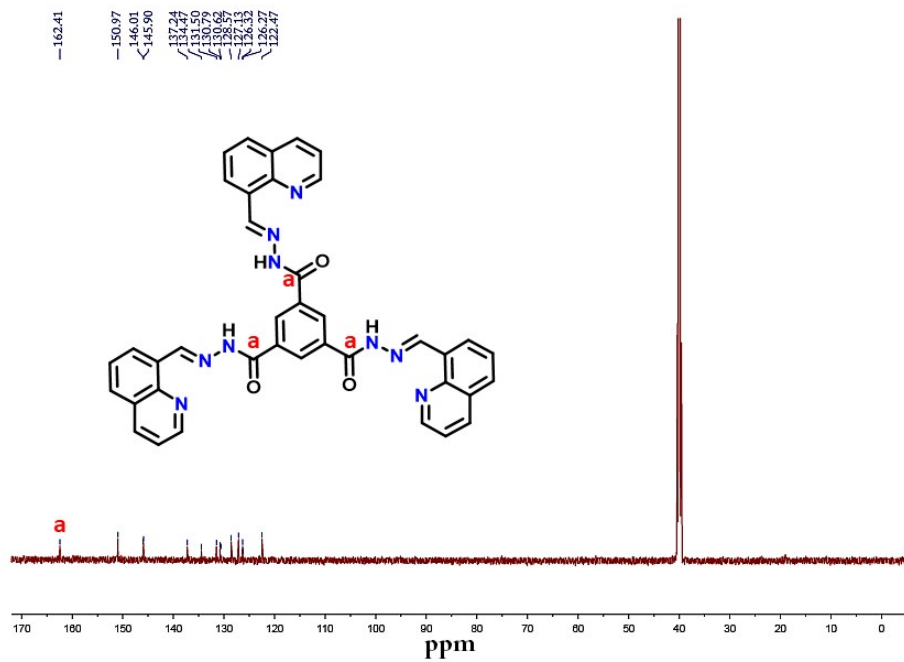


Figure S4. ^{13}C NMR spectrum of **TRI-QUI** in $\text{DMSO-}d_6$.

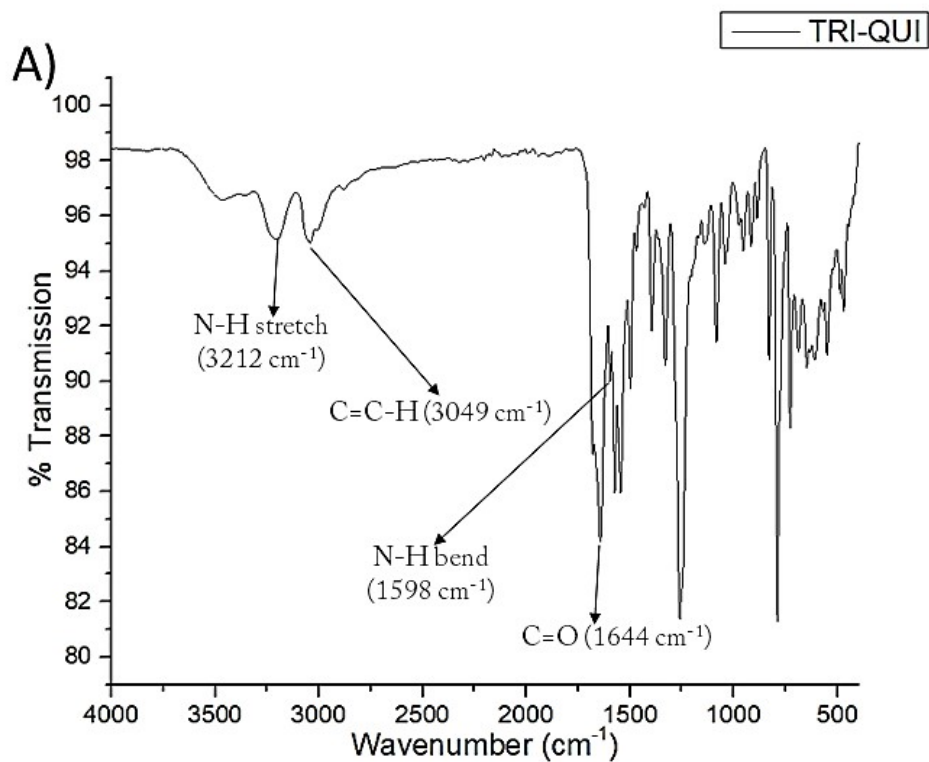


Figure S5. FTIR spectra of **TRI-QUI**.

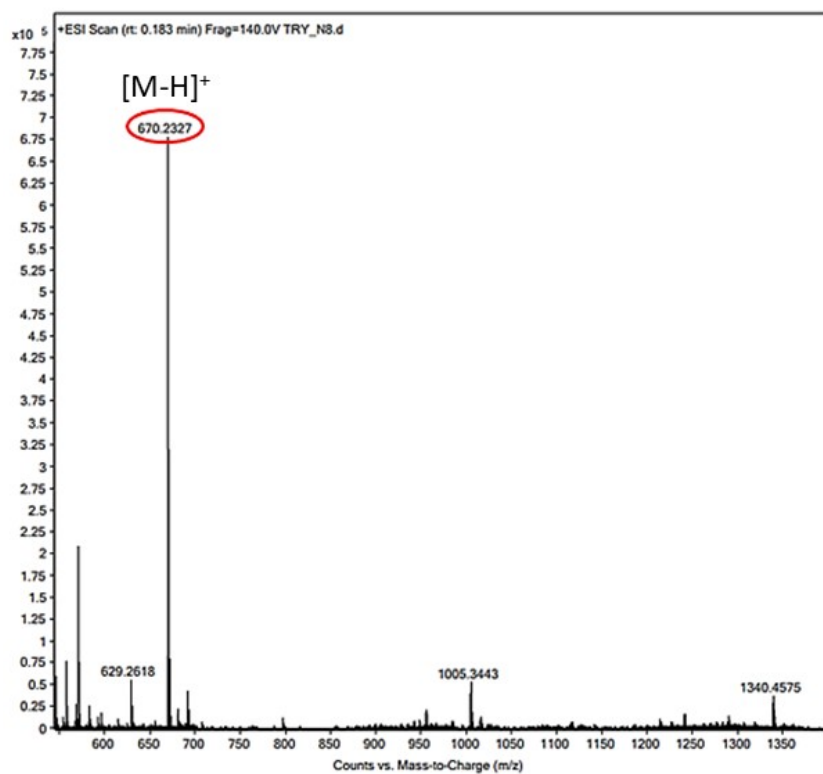


Figure S6. HRMS of TRI-QUI.

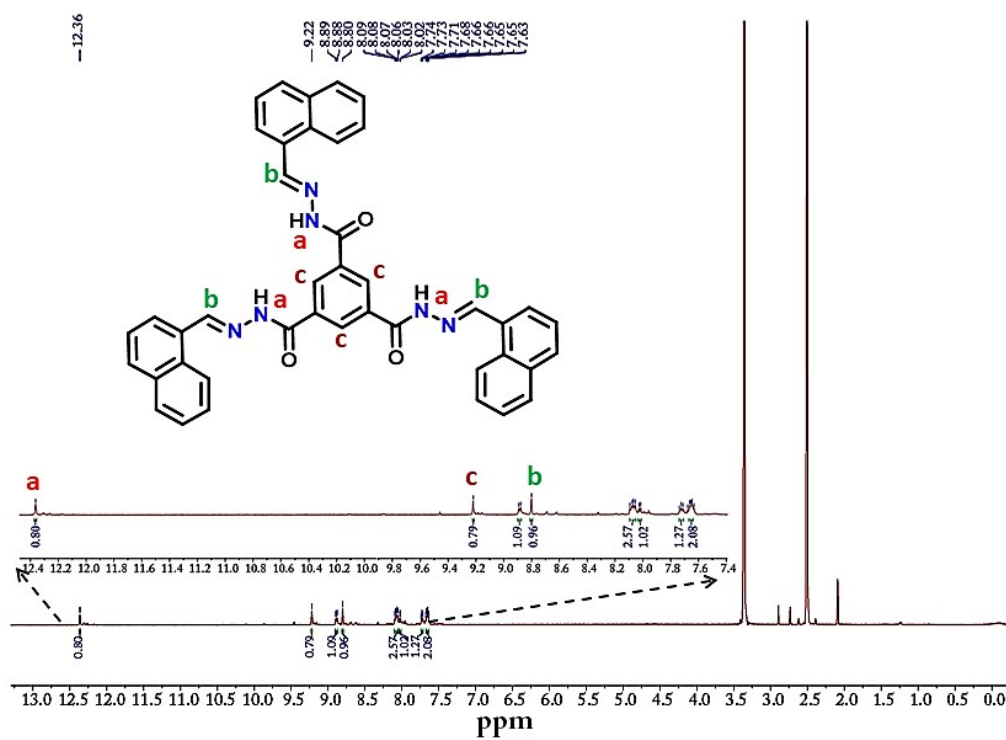


Figure S7. ^1H NMR spectrum of TRI-NAP in $\text{DMSO-}d_6$.

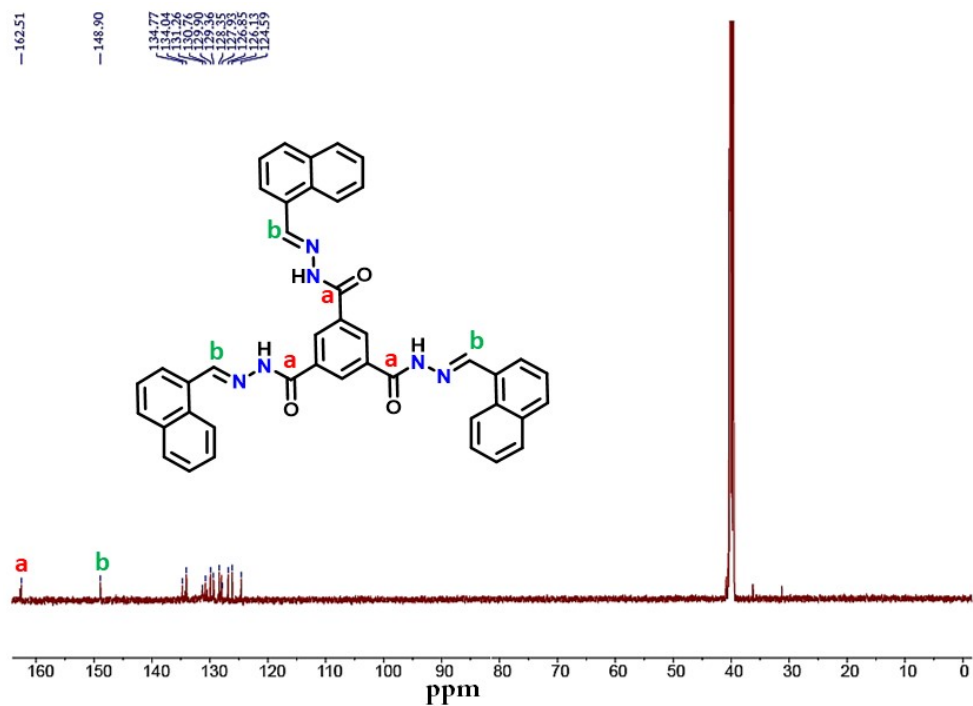


Figure S8. ^{13}C NMR spectrum of **TRI-NAP** in $\text{DMSO-}d_6$.

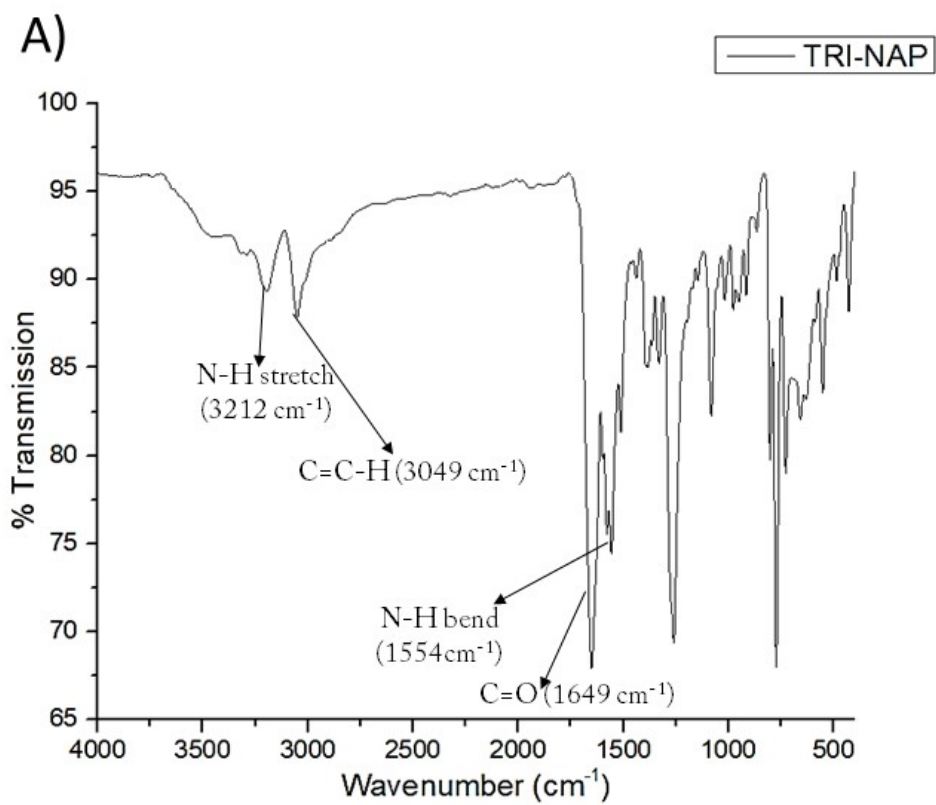


Figure S9. FTIR spectra of **TRI-NAP**.

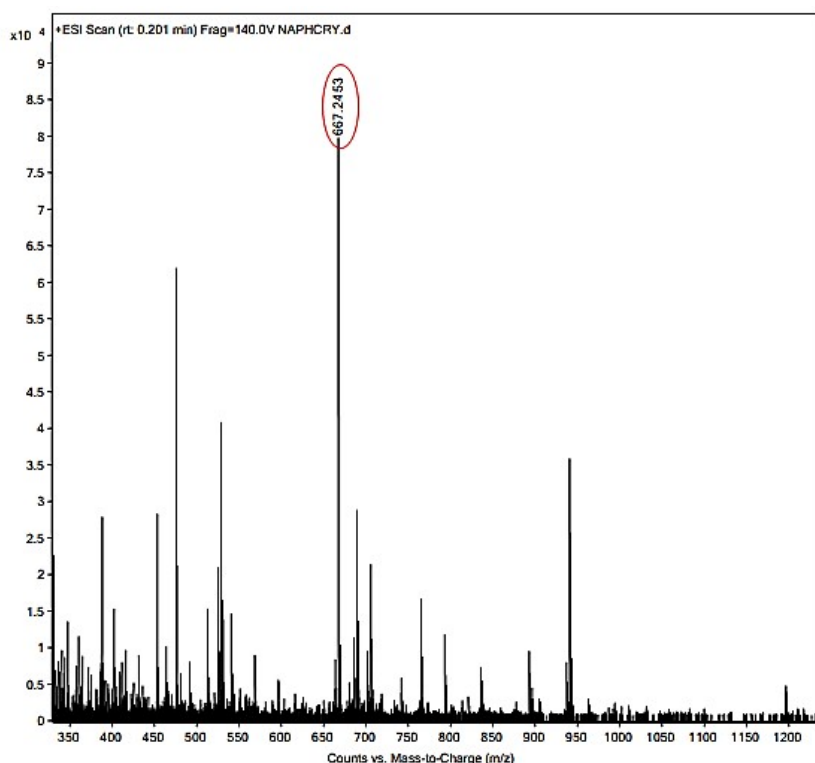


Figure S10. HRMS of TRI-QUI.

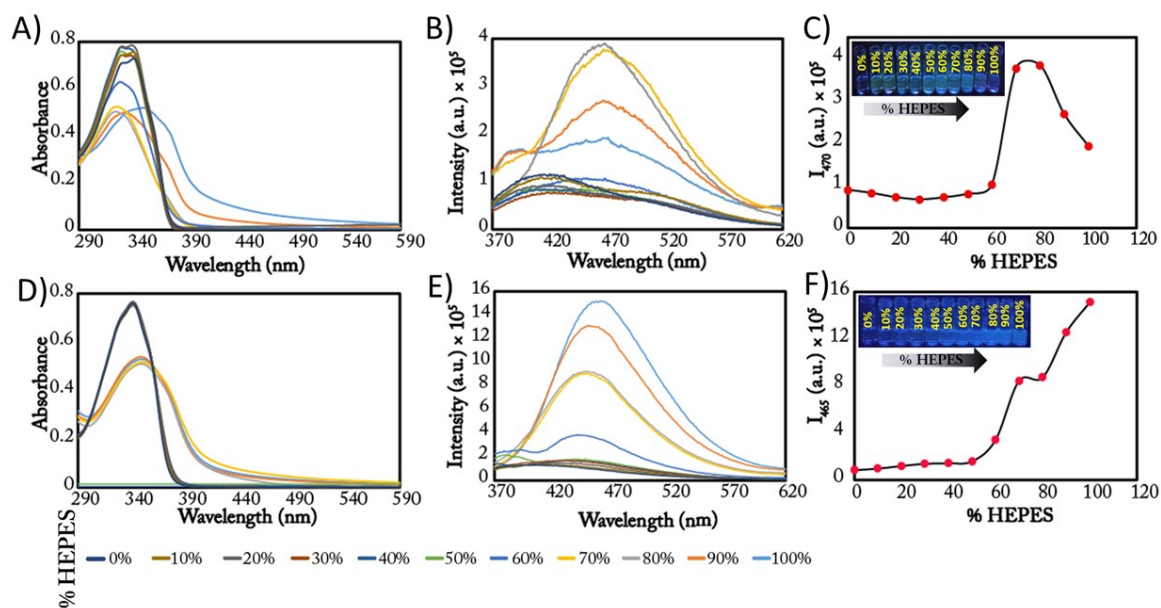


Figure S11. Absorbance spectrum of (A) TRI-QUI, and (D) TRI-NAP in DMF and HEPES. Emission spectroscopy with increasing percentages of HEPES in DMF of (B) TRI-QUI, and (E) TRI-NAP. Plot of percentage of water vs emission intensity of (C) TRI-QUI and (F) TRI-NAP [INSET: Visual illustration of the AIE activity of TRI-QUI (20 μM) and TRI-NAP (20 μM) under a 365 nm UV lamp].

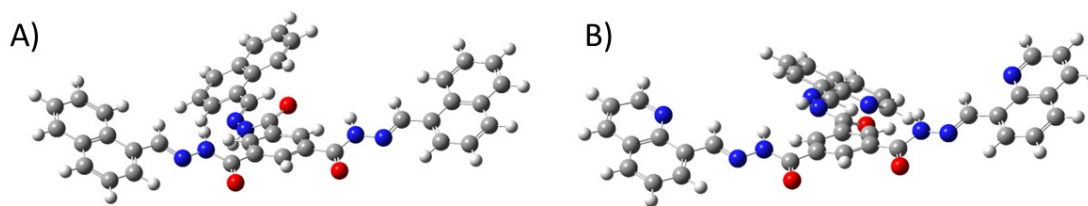


Figure S12. DFT optimized structures of both the probes.

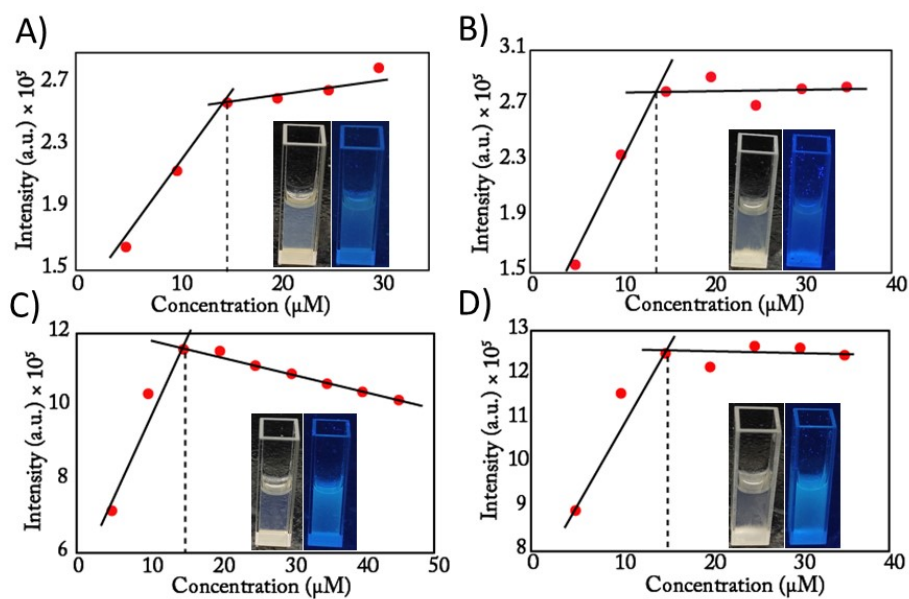
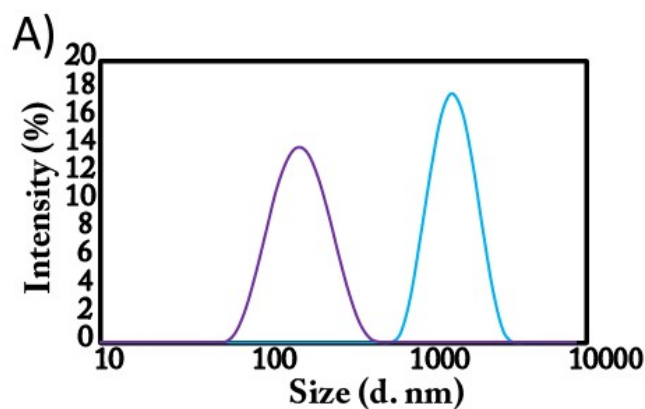


Figure S13. Critical aggregation constant of **TRI-QUI** in A) H₂O, B) HEPES, and of **TRI-NAP** in C) H₂O, D) HEPES.



SAMPLES	H ₂ O	
	Z-Avg (d. nm)	PDI
 TRI-QUI	1303	0.164
 TRI-NAP	155.9	0.143

Figure S14. DLS output of **TRI-QUI** in 80% H₂O and **TRI-NAP** in 100% H₂O.

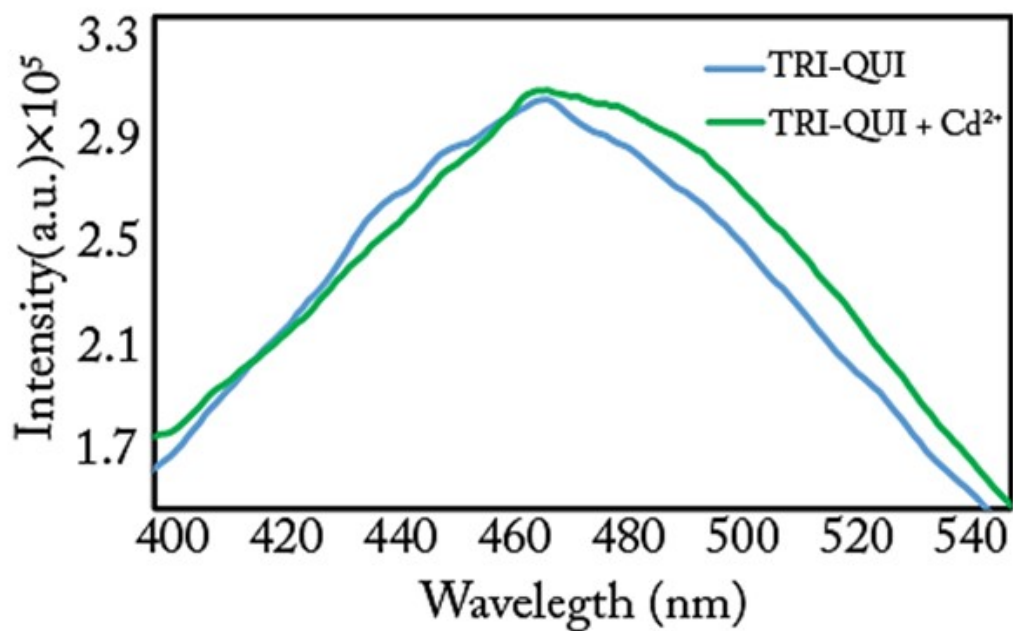


Figure S15. Sensing of Cd^{2+} by TRI-QUI in HEPES (enlarged view).

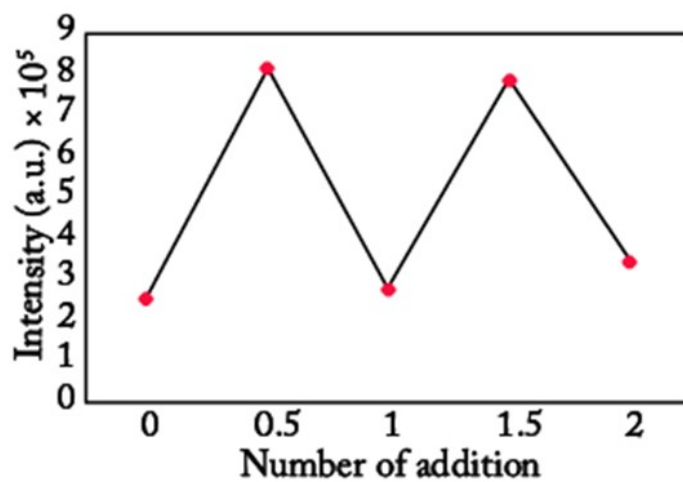


Figure S16. Sensing of Cd^{2+} by TRI-QUI in HEPES (enlarged view).

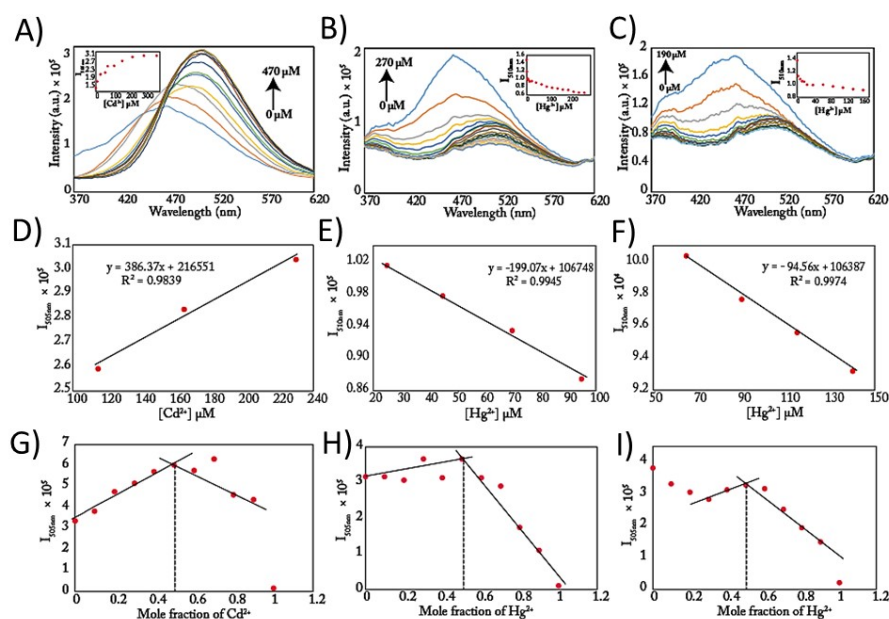


Figure S17. Emission intensity profile depicting the titration of **TRI-QUI** with Cd²⁺ A) in water, with Hg²⁺ B) in H₂O and C) in HEPES, fluorescence emission intensity of **TRI-QUI** vs. D) Cd²⁺ concentration E), F) Hg²⁺ concentration to calculate the limit of detection (LOD), Job's plot of **TRI-QUI** with G) Cd²⁺ H), I) Hg²⁺.

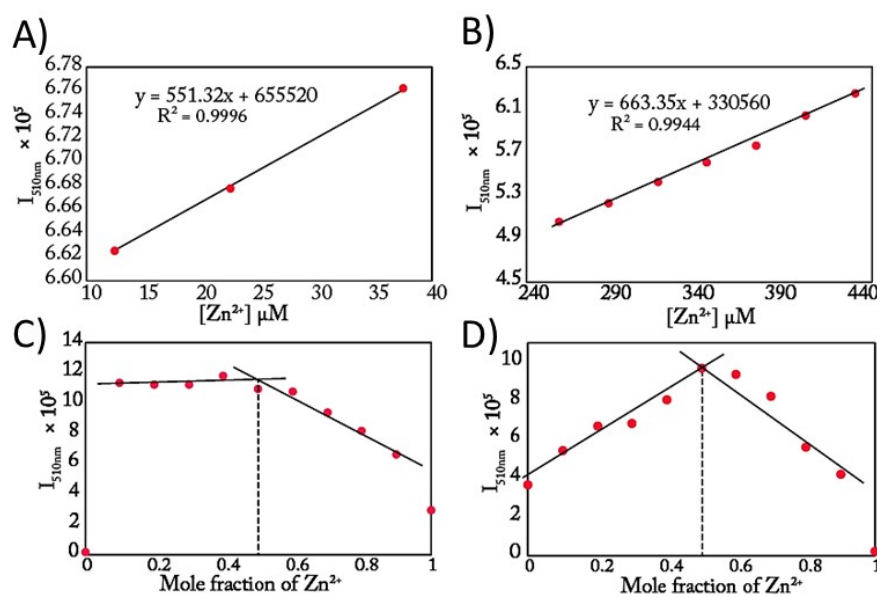


Figure S18. The fluorescence emission intensity of **TRI-QUI** vs. Zn²⁺ concentration A) in water and B) in HEPES to calculate the limit of detection (LOD), Job's plot of **TRI-QUI** with mole fraction of Zn²⁺ A) in water and A) in HEPES.

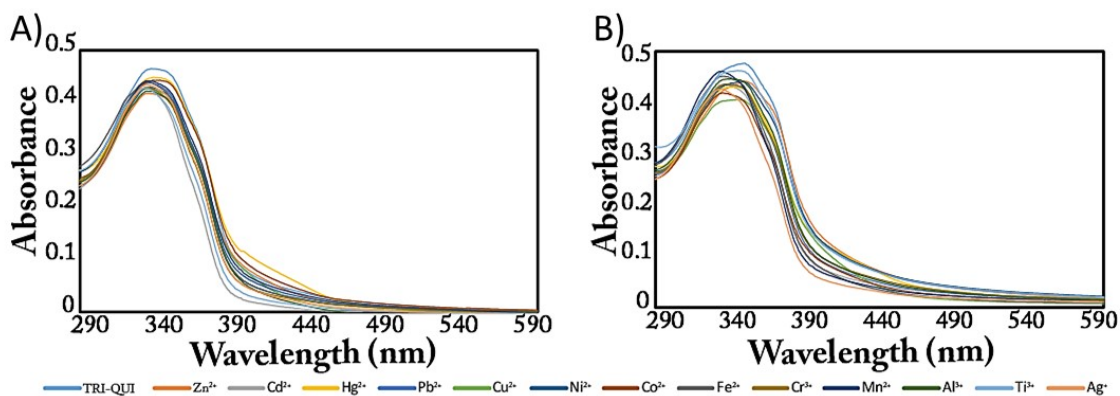
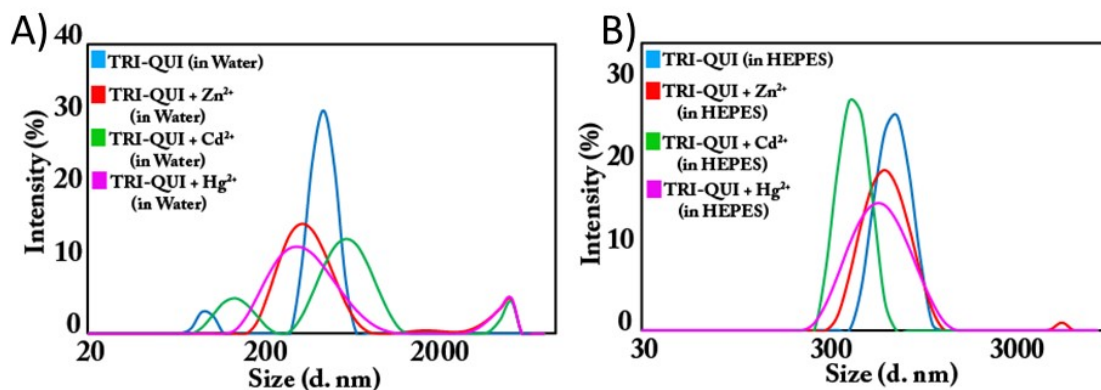


Figure S19. UV-Vis Sensing of metal ions by **TRI-QUI** A) in water and B) in HEPES.



SAMPLES	H ₂ O		HEPES	
	Z-Avg (d. nm)	PDI	Z-Avg (d. nm)	PDI
TRI-QUI	828.9	0.802	907.2	0.519
TRI-QUI + Zn ²⁺	462.7	0.398	641.7	0.249
TRI-QUI + Cd ²⁺	483.6	0.708	703.8	0.651
TRI-QUI + Hg ²⁺	419.6	0.409	509.9	0.270

Figure S20. DLS output of **TRI-QUI** in the presence of Zn²⁺, Cd²⁺, and Hg²⁺ A) in water and B) in HEPES.

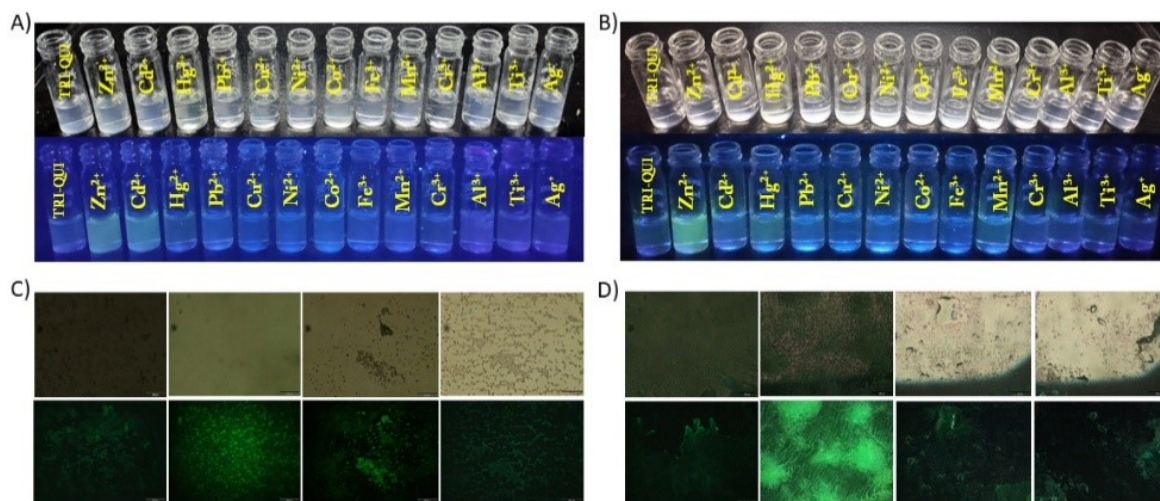


Figure S21. Vial images of **TRI-QUI** in the presence of different metal ions A) in water, B) in HEPES, and fluorescence microscope images of **TRI-QUI** in the presence of Zn²⁺, Cd²⁺, and Hg²⁺ respectively C) in water and D) in HEPES.

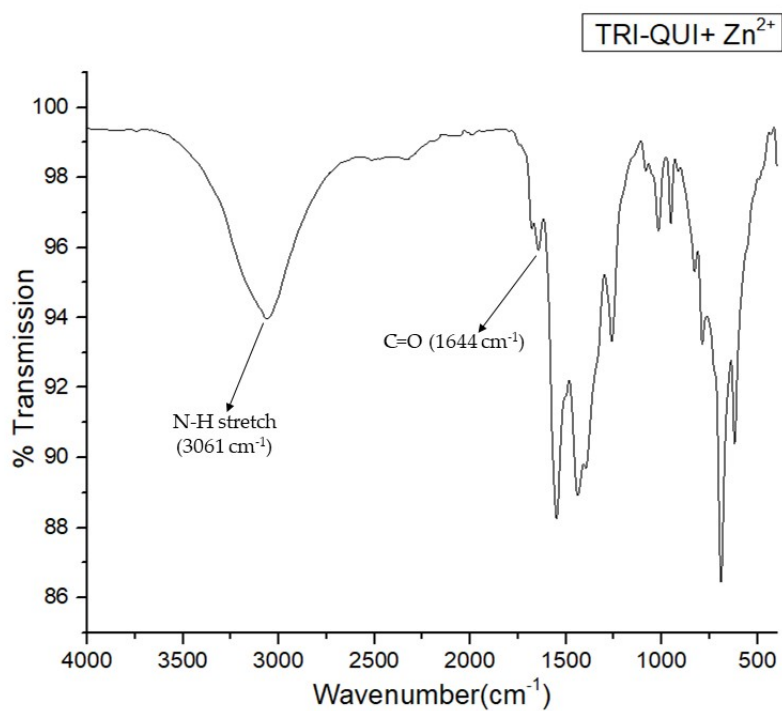


Figure S22. FT-IR spectra of **TRI-QUI** in the presence of Zn²⁺.

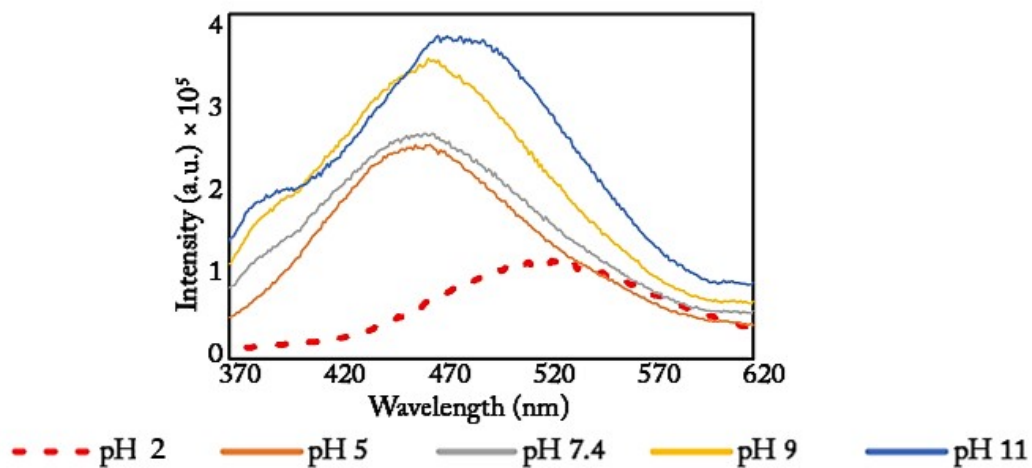


Figure S23. Fluorescence spectra of TRI-QUI in different pH.

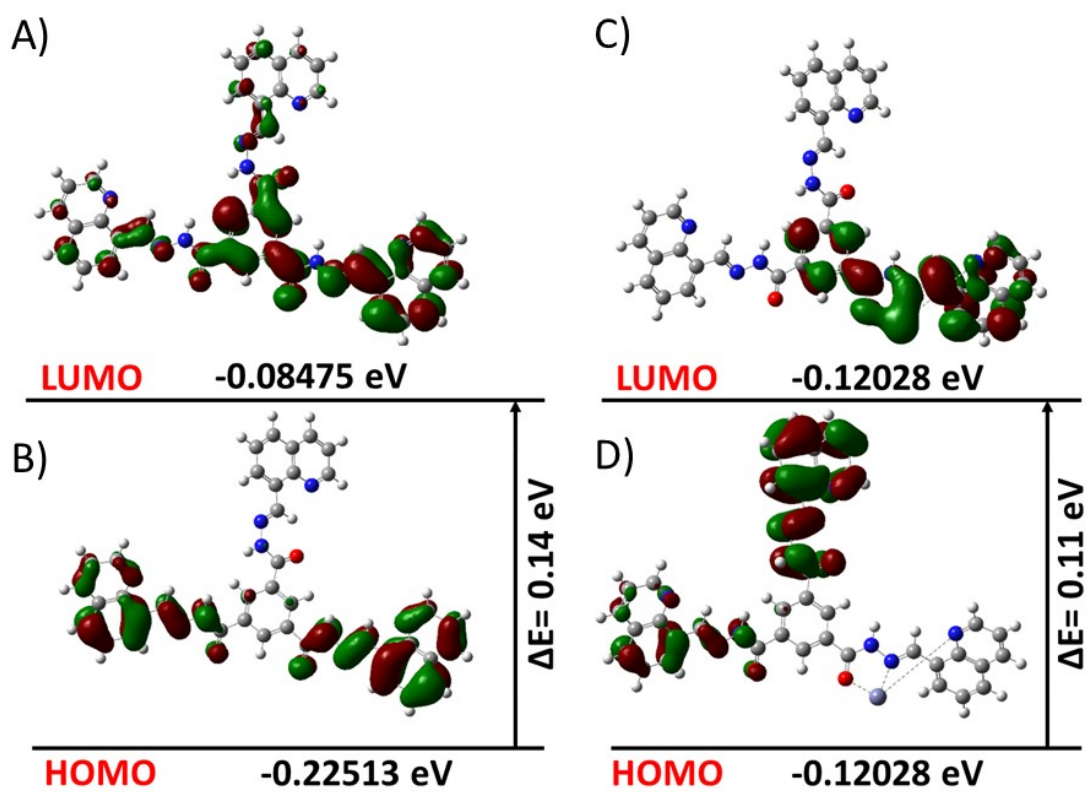


Figure S24. HOMO and LUMO of TRI-QUI in absence A), B) and in presence C), D) of Zn^{2+} .

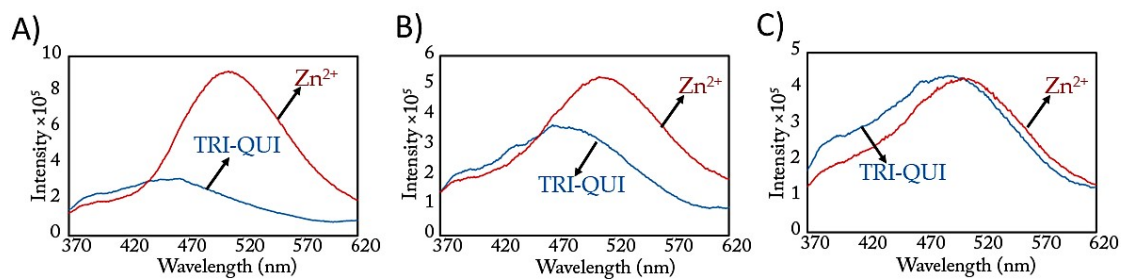


Figure S25. Sensing of Zn^{2+} in real water samples A) milli Q water B) drinking water and C) tap water.

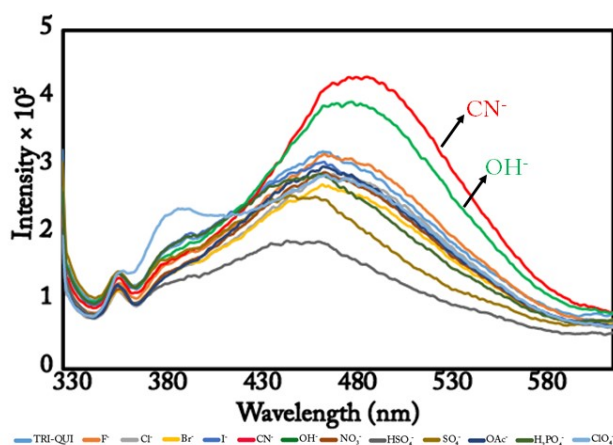


Figure S26. Anion sensing by TRI-QUI in water.

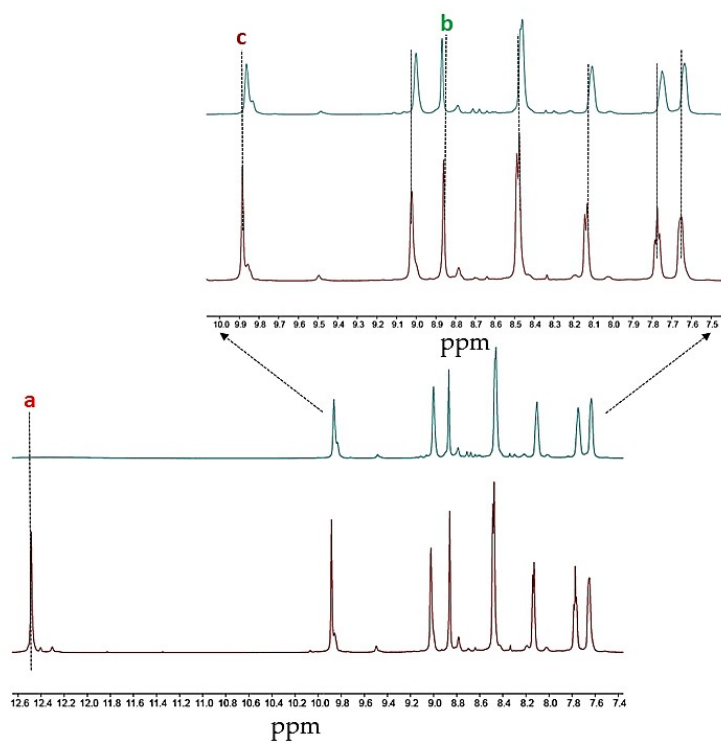


Figure S27. 1H NMR spectra of TRI-QUI in the presence of excess of CN^- .

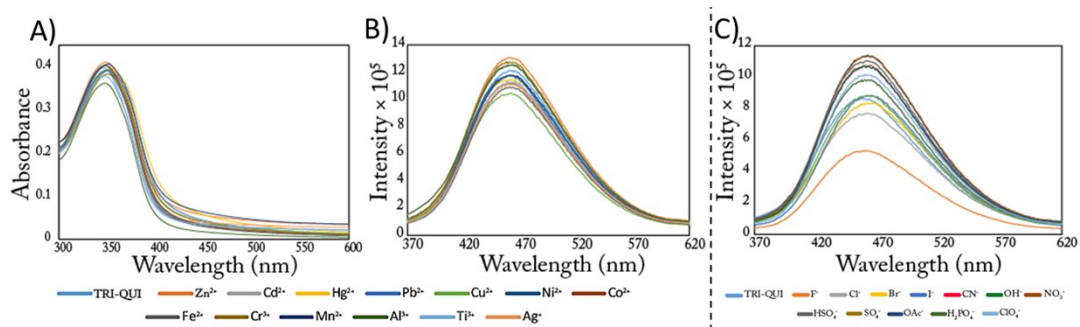


Figure S28. A) UV-Vis sensing of metal ions, B) fluorescence sensing of metal ions, and C) fluorescence sensing of anions by **TRI-NAP** in water.

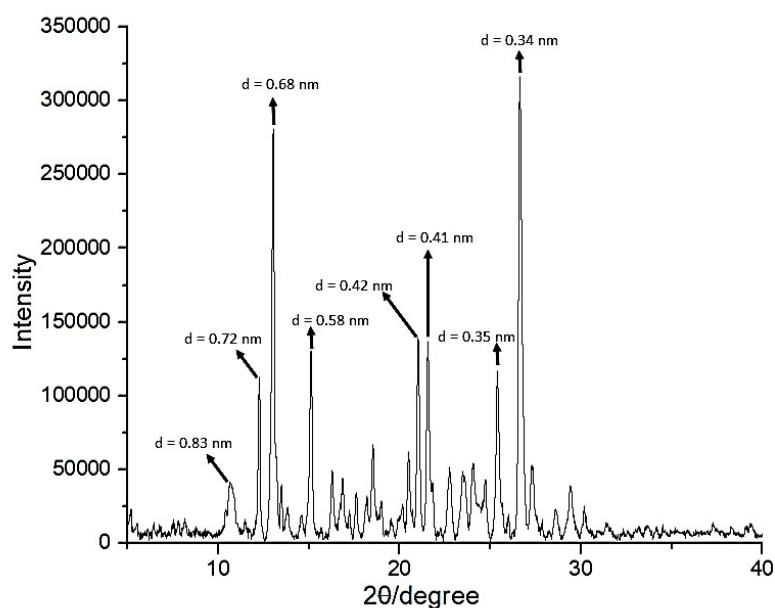


Figure S29. Powder XRD spectra of xerogel **TRI-QUI**.

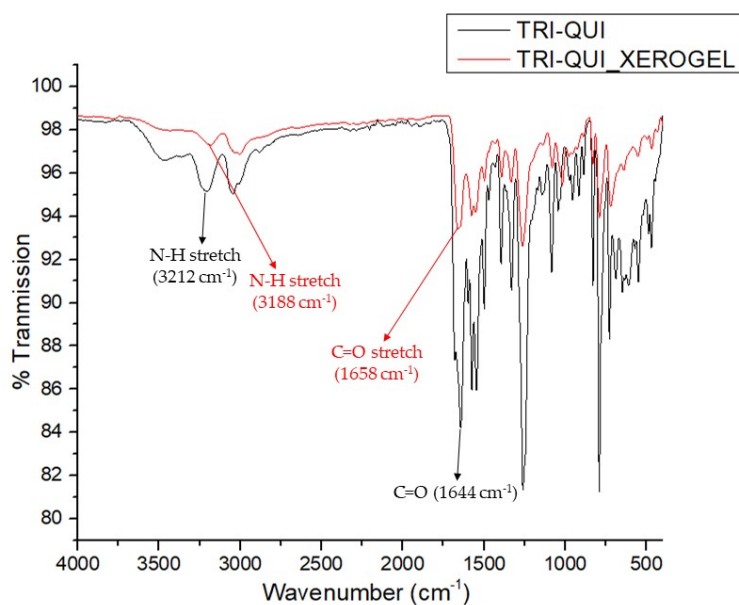


Figure S30. FT-IR spectra of xerogel **TRI-QUI**.

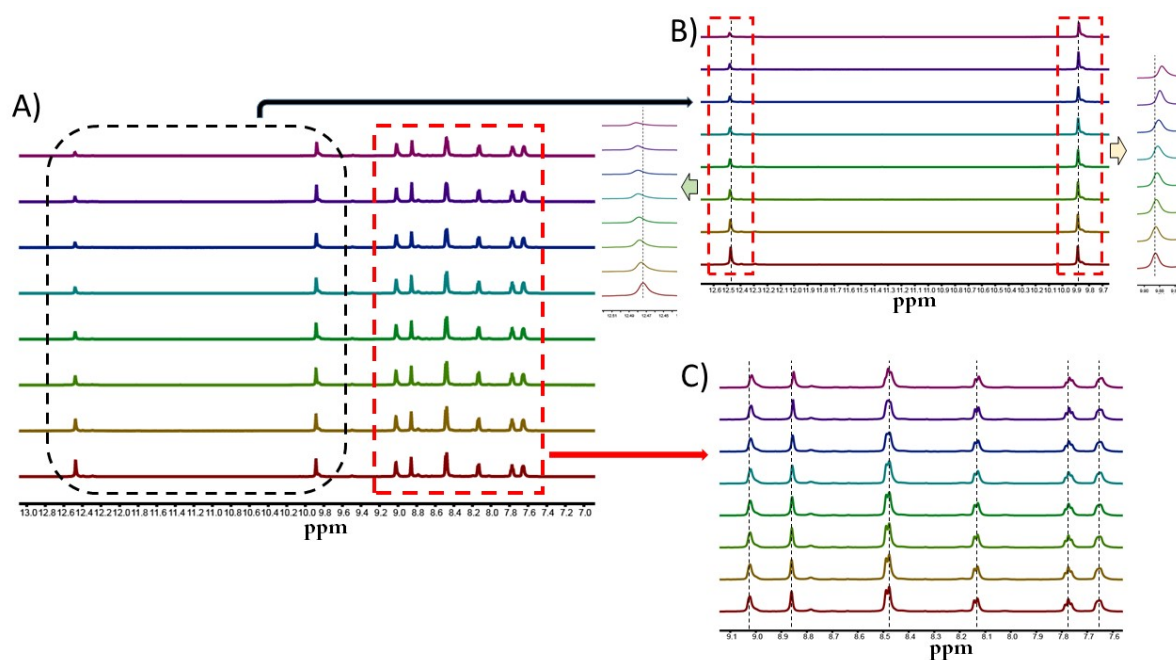


Figure S31. ^1H NMR spectra of TRI-QUI in $\text{DMSO-}d_6$ with increasing content of D_2O .

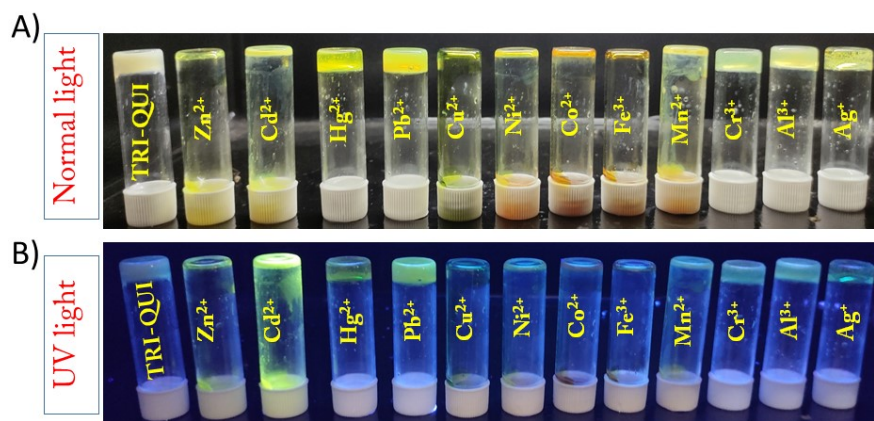


Figure S32. TRI-QUI gel formed in $\text{DMSO-H}_2\text{O}$ (2: 3, v/v) in the presence of different metal ions A) in normal light and B) in UV light.

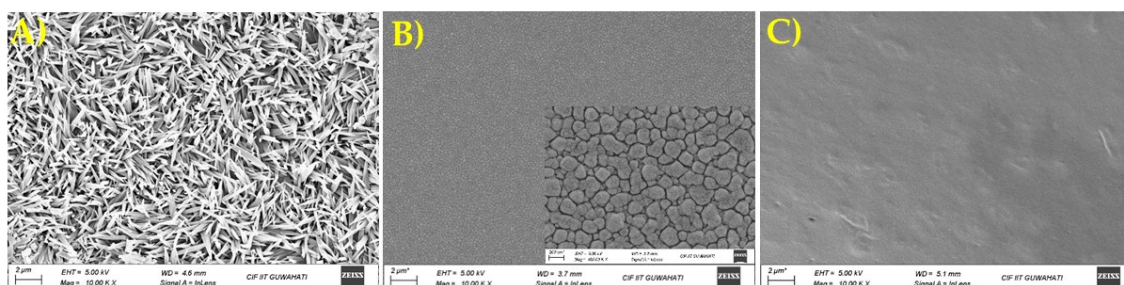


Figure S33. FESEM images of A) TRI-QUI xerogel obtained from $\text{DMSO-H}_2\text{O}$ (2: 3, v/v), B) TRI-QUI+ Ag^{2+} xerogel obtained from $\text{DMSO-H}_2\text{O}$ (2: 3, v/v), F) TRI-QUI+ SO_4^{2-} xerogel obtained from $\text{DMSO-H}_2\text{O}$ (2: 3, v/v).

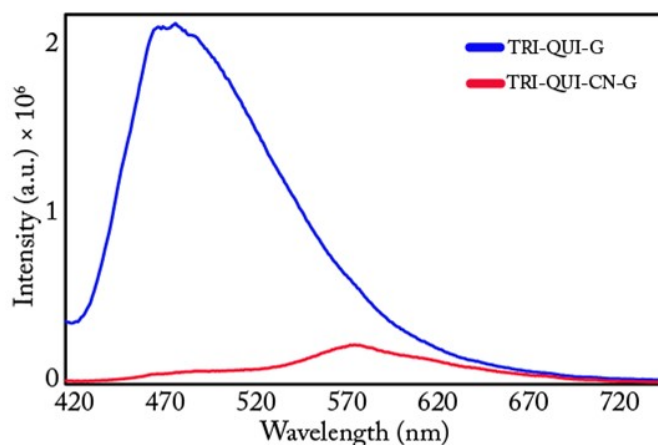


Figure S34. Fluorescence spectra of TRI-QUI gel formed in DMSO-H₂O (2: 3, v/v) and TRI-QUI gel formed in DMSO-H₂O (2: 3, v/v) formed in the presence of CN⁻.

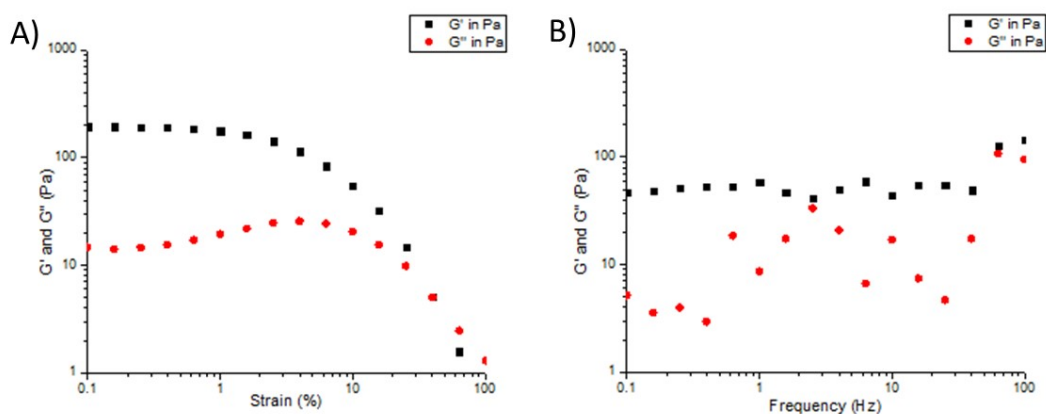


Figure S35. A) Amplitude sweep and B) Frequency sweep of TRI-NAP organogel DMSO-H₂O (2: 3, v/v).

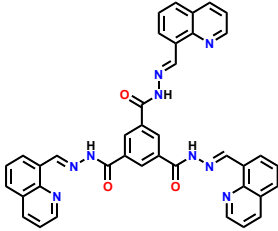
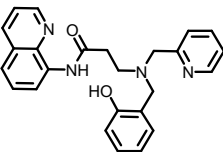
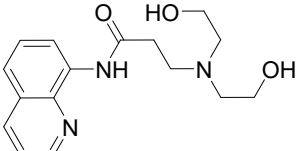
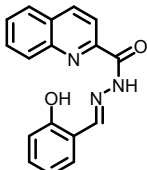
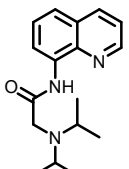
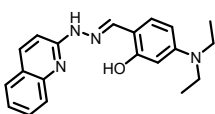
Table S1. Hydrogen bonding distances (Å) and Bond angles (°) in TRI-QUI.

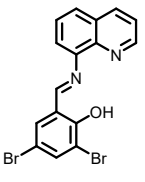
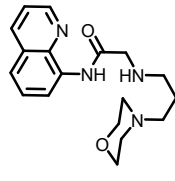
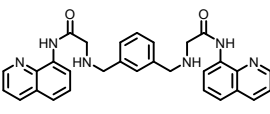
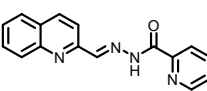
Ligand	D H...A	d(D...H)/Å	d(H...A)/Å	d(D...A)/Å	<D-H...A/	Symmetry codes
TRI-QUI	N1-H1N...N5	0.79 (4)	2.51 (4)	3.189 (5)	145 (4)	-x, 1-y, 1-z
	O4-H4B...N6	1.02 (10)	2.07 (10)	3.065 (6)	165 (8)	x, y, z
	N4-H4N...O1	0.74 (4)	2.21 (4)	2.931 (5)	164 (4)	1-x, 1-y, 1-z
	N7-H7N...O4	0.82 (5)	2.27 (5)	3.055 (6)	162 (5)	1-x, 1-y, 1-z
	C6-H6...O4	0.93	2.60	3.354 (6)	139	1-x, 1-y, 1-z
	C23-H23...O1	0.93	2.56	3.369 (5)	146	-1+x, 1+y, z
	C30-H30...O3	0.93	2.52	3.426 (6)	164	-x, 1-y, 1-z
	C39-H39...O2	0.93	2.48	3.337 (6)	154	x, y, -1+z

Table S2. Table for LOD and binding constant calculation in H₂O and HEPES.

Metal	MEDIUM	LOD	BINDING STOICHIOMETRY
Zn ²⁺	H ₂ O	14.33 μM	1:1
	HEPES	6.45 μM	1:1
Cd ²⁺	H ₂ O	20.44 μM	1:1
Hg ²⁺	H ₂ O	39.68 μM	1:1
	HEPES	45.26 μM	1:1

Table S3. Table for LOD and binding constant calculation in H₂O and HEPES.

Sl. No.	References	Structure of probe	Solvent system	LOD (μM)
1.	Present work		0.1M HEPES buffer	6.45
2.	Sensors and Actuators B: Chemical, 2015, 213, 268-275		10 mM HEPES, pH 7.4, 1:1 acetonitrile/buffer	8.14 × 10 ⁻³
3.	RSC Advances, 2015,5, 60796-60803		10 mM bis-tris buffer	4.48
4.	Sensors and Actuators B 2016, 234, 616-624		MeOH-HEPES buffer (3/7, v/v, pH 7.4)	2.1 × 10 ⁻²
5.	Dyes and Pigments 2018, 158, 312-318		MeOH-Tris buffer (1/1, v/v, pH 7.2)	4.1 × 10 ⁻²
6.	New J. Chem., 2019,43, 7320-7328		buffer/DMF mixture (7:3)	0.08

7.	Dalton Transaction, 2020, 49, 4758-4773		10 mM HEPES buffer	1.39×10^{-1}
8.	New Journal of Chemistry, 2020, 44, 442-449		bis-tris buffer	0.29
9.	Journal of Fluorescence, 2020, 30, 347-356		DMSO/bis-tris buffer (1:1)	0.53
10.	Microchemical Journal 2021, 160, 105776		DMSO/HEPES buffer solution (v/v = 3/2, HEPES 10 mM, pH 7.4)	72×10^{-3}

References

1. S. Sharma , M. Kumari and N. Singh , *Soft Matter*, 2020, **16**, 6532-6538.
2. Apex 3; Bruker AXS Inc.: 2016.
3. Apex 4. Bruker AXS Inc.; 2016.
4. SMART, SAINT, and XPREP; Siemens Analytical X-ray Instruments Inc.: 1995.
5. G. M. Sheldrick, SADABS, Program for Area Detector Adsorption Correction; Institute for Inorganic Chemistry, University of Göttingen: 1996.
6. G. M. Sheldrick, Crystal structure refinement with SHELXL. *Acta Crystallogr., Sect. C: Struct. Chem.*, 2015, 71, 3.
7. C. F. Macrae, I. Sovago, S. J. Cottrell, P. T. A. Galek, P. McCabe, E. Pidcock, M. Platings, G. P. Shields, J. S. Stevens, M. Towler and P. A. Wood, Mercury 4.0: from visualization to analysis, design and prediction. *J. Appl. Crystallogr.*, 2020, 53, 226.